



## **Proportioning energy-dissipating members in strongback braced frames**

Peter C. Talley<sup>1</sup>, Mark D. Denavit<sup>2</sup>, Nicholas E. Wierschem<sup>3</sup>

### **Abstract**

Many structural systems are susceptible to soft-story instabilities during earthquakes that are life-threatening and can lead to damage that is too costly to repair. One way to mitigate damage and reduce the potential for soft-story instability is through the addition of an elastic spine that distributes drifts across the height of a structure. One such system is the strongback braced frame, which replaces one side of a buckling-restrained braced frame with a strongback truss. With the strongback providing vertical continuity, an expanded design space is made available for the arrangement of buckling-restrained braces (BRBs) or other energy-dissipating members. An example of this expanded design space is that a designer could opt to not include BRBs at every story. Methods for proportioning the energy-dissipating resistance in strongback braced frames have been proposed. However, most methods don't allow exploitation of the full design space. The objective of this work is to propose and evaluate a potential method of proportioning energy-dissipating members for arbitrary vertical arrangements within strongback braced frames. For a prototypical building, the BRBs are designed in various configurations using existing methods and with the new method. Nonlinear time history analyses of the resulting designs coupled with a rigid strongback are performed and the results are compared. The impacts of overstrength and  $P-\Delta$  effects are quantified. The findings support the proposed method of BRB design that enables exploration of the wide design space made available by the strongback.

### **1. Introduction**

Many steel structures are susceptible to soft-story instabilities, whereby a single story yields and proceeds to accumulate damage without engaging the resistance of the rest of the structure. One approach for alleviating this undesirable failure mode is through the use of a stiff elastic spine that runs the height of the structure and distributes demand vertically. One system that utilizes a spine is the strongback braced frame (SBF). In this system, the spine consists of a stiff vertical steel truss pinned at its base, to which are attached buckling-restrained braces (BRBs) that provide lateral resistance and energy dissipation capacity (Lai and Mahin 2014; Simpson 2018).

---

<sup>1</sup> Graduate Research Assistant, University of Tennessee, Knoxville, <ptalley2@vols.utk.edu>

<sup>2</sup> Assistant Professor, University of Tennessee, Knoxville, <mdenavit@utk.edu>

<sup>3</sup> Associate Professor, University of Tennessee, Knoxville, <nwiersch@utk.edu>

Design of SBFs and other spine frame systems currently requires extensive analysis, up to and including design by nonlinear time history analysis. Design by nonlinear time history analysis is time-consuming and requires expertise beyond what is required for typical seismic design of buildings. If SBFs can only be designed using advanced methods, the use of SBFs will be limited, and the potential benefits of the system in increased collapse resistance and resilience will not be realized. However, spine frame systems, including the SBF, have some unique design considerations which have yet to be addressed in standardized approaches. One consideration is the additional higher mode demands caused by the addition of the spine, which are not captured by standardized seismic design methods such as the equivalent lateral force (ELF) procedure defined in ASCE 7 (ASCE 2016), even when supplemented with AISC 341 (AISC 2016) capacity design. Accounting for these demands is necessary to design the spine, however when designing the primary lateral resistance—i.e., the BRBs—it is common to assume that the first-mode demands are sufficient to yield the structure/form a plastic mechanism.

While a major motivation of a SBF is to preclude soft-story instabilities, the ability of the strongback to distribute deformations also opens a design space for the lateral and energy dissipating resistance. BRBs are necessary as the strongback is pinned at the base and provides no lateral capacity on its own. However, unlike a buckling restrained braced frame, BRBs are not required at each story, as the strongback enables redistribution of forces to other stories. This redistribution also means that the strongback provides a mechanism for inherent redundancy within a single frame, allowing use of 1.0 for the ASCE 7 redundancy factor  $\rho$  in some cases (Panian et al. 2017). This design space has not been fully explored, nor have efficient methods of design been developed to allow engineers to take advantage of it.

The objective of this work is to evaluate several different methods for sizing BRBs in SBFs, including a new approach described herein based on the formation of a plastic mechanism. The paper is organized as follows. Section 2 introduces the different methods for sizing BRBs that will be evaluated. Section 3 describes the approach used to evaluate the performance of the resulting designs. Section 4 presents and discusses the results from the analysis. Section 5 presents the conclusions.

## **2. Different Methods for Sizing BRBs**

Four methods for the initial sizing of BRBs are considered in this work: (1) proportional to ELF demands from an elastic analysis of the frame; (2) proportional to ELF demands, assuming that the BRBs resist the full story shear at each level; (3) a uniform BRB size, with each level designed to resist a constant factor of the base shear; and (4) a new approach based on overturning resistance at the capacity limit state.

The first method for proportioning BRBs to be evaluated in this work, referred to here as the *equivalent lateral force* method, is based on the demands from an elastic analysis of the frame under ELF demands. The size of the BRBs will generally decrease in higher stories, as the lower stories will be subject to larger forces. No accounting for post-yield redistribution of forces by the strongback is performed. This method is straightforward, but requires a complete model of the frame and iterative design using elastic analysis.

Alternatively, the BRBs may be sized without an analysis of the whole frame by assuming they resist the full story shear at each level that result from the ELF demands. In this method, referred to here as the *proportional shear* method, the required steel core area of story  $x$ ,  $A_{sc,x}$ , assuming a single BRB at each level, is given by

$$A_{sc,x} \geq \frac{V_x}{\phi F_{ysc} \cos \alpha_x} \quad (1)$$

where  $V_x$  is the story shear tributary to the frame at story  $x$ ,  $F_{ysc}$  is the nominal yield strength of the steel core,  $\phi$  is the resistance factor for brace core yielding (0.9), and  $\alpha_x$  is the brace angle at story  $x$ . The design strength used here,  $\phi F_{ysc} A_{sc}$ , is taken from the buckling-restrained brace frame provisions of AISC 341-16 (AISC 2016).

The third method, referred to in this work as the *constant shear* method, takes advantage of the strongback's ability to redistribute forces. Several authors (Panian et al. 2017; Simpson 2018) have, instead of proportional BRB sizes, used uniform BRB sizing, with the strongback enabling the BRBs in the upper stories to develop their full capacity. Use of the same size BRB in all stories can reduce cost and provide other constructability benefits. Simpson (2018) proposed a simple method for sizing the BRBs where each story is designed for 80% of the total base shear,  $V$ . This method is simple and effective, but cannot be applied to building configurations that do not feature a full complement of BRBs. The required area due to this story shear is still dependent on the angle of the brace in the story. In this work, to produce a single BRB size, the average of the required area is used. The required area can be formulated as:

$$A_{sc} \geq \frac{1}{n} \sum_{x=1}^n \frac{0.8V}{\phi F_{ysc} \cos \alpha_x} \quad (2)$$

The fourth method, developed in this work and referred to as the *overturning* method, is based on evaluating the structure at the capacity limit state. The goals for development of this method were (1) flexibility in choice of BRB size (proportional, uniform, or other); (2) flexibility in choice of BRB location (e.g., skipping stories); and (3) simplicity of implementation. In this work, the method is used to produce a single BRB size, but not limited to structures with a “full complement” of BRBs, as no assumption about the story shear distribution is made up front. The primary assumption is that the first mode forces cause the formation of a complete plastic mechanism of the system.

The general approach is to assume that the strongback is rigid and the other beams and columns are pinned. The BRBs are replaced with corresponding capacity forces assuming that the demand is pushing to the left or to the right. Since the BRBs are not designed yet, these capacity forces are defined in terms of the unknown core area. Loads are applied to the frame as a factor,  $\gamma$ , times the forces from the equivalent lateral force (ELF) method. Determination of the appropriate load scaling factor  $\gamma$  is an objective of this work. An example frame with capacity force and ELF forces is shown in Fig. 1(a). A free body diagram of the strongback for this frame is shown in Fig. 1(b). An equation of equilibrium can be formed by taking the sum of the moments about the base of the strongback and used to solve for the core area required to achieve equilibrium.

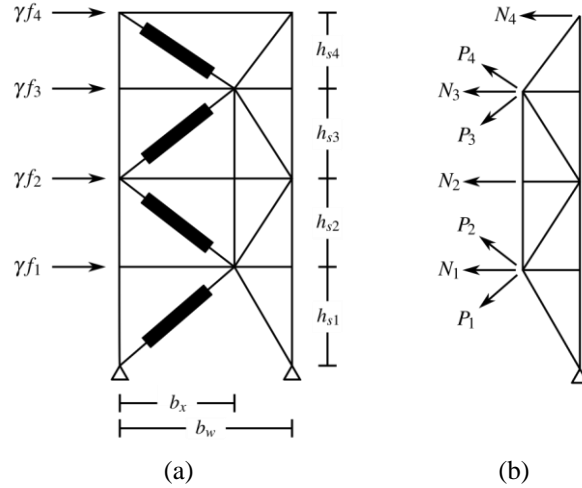


Figure 1: (a) Example frame and ELF forces for overturning procedure; (b) Free-body diagram of the strongback portion of the frame

For basic configurations, the free-body diagram in Fig. 1(b) can be generalized. The numbering scheme used to develop the general equation is shown in Fig. 2. To account for an arbitrary layout of braces, a numbering scheme is used where “rising” braces are notated by 1 and “falling” braces are notated by 2.

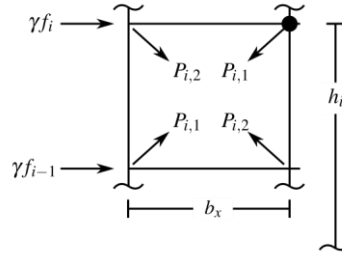


Figure 2: Numbering scheme for overturning procedure

The internal force in the beam at story  $i$ ,  $N_i$ , can thus be written as

$$N_i = -\left(P_{i,2} \cos \alpha_i + P_{i+1,1} \cos \alpha_{i+1} + \gamma f_i\right) \quad (3)$$

where  $f_i$  is the force at floor  $i$  from the equivalent lateral force procedure and  $P_i$  is the force in the buckling-restrained brace at capacity:

$$\begin{aligned} P_i \text{ (tension)} &= F_t A_{sc,i} \\ P_i \text{ (compression)} &= -F_c A_{sc,i} \end{aligned} \quad (4)$$

where  $F_t$  is the capacity-limited stress in tension and  $F_c$  is the capacity-limited stress in compression, both from AISC 341-16. If a brace is not present, the respective  $P_i$  term is taken as zero. After performing the cut shown in Fig. 1(b), the  $x$ - and  $y$ -components of the resultant force (excluding the overturning force  $\gamma f_i$ ) at the top right of each story (indicated by the dot in Fig. 2) are then

$$\begin{aligned}
R_{x,i} &= (P_{i,1} - P_{i,2}) \cos \alpha_i - (P_{i+1,1} - P_{i+1,2}) \cos \alpha_{i+1} \\
R_{y,i} &= P_{i,1} \sin \alpha_i - P_{i+1,2} \sin \alpha_{i+1}
\end{aligned} \tag{5}$$

If all braces have the same core area,  $A_{sc}$ , these may be re-written in terms of stress:

$$\begin{aligned}
R_{x,i} &= A_{sc} X_i = A_{sc} \left[ (F_{i,1} - F_{i,2}) \cos \alpha_i - (F_{i+1,1} - F_{i+1,2}) \cos \alpha_{i+1} \right] \\
R_{y,i} &= A_{sc} Y_i = A_{sc} (F_{i,1} \sin \alpha_i - F_{i+1,2} \sin \alpha_{i+1})
\end{aligned} \tag{6}$$

where  $F_{i,1}$  and  $F_{i,2}$  have the same numbering convention as their respective  $P_i$  terms. By summing the moments around the base of the strongback, the resistance of the frame to overturning,  $M_n$ , can be calculated as shown in Eq. 7.

$$M_n = A_{sc} \sum_{i=1}^N X_i h_i + Y_i (b_w - b_x) \tag{7}$$

where  $h_i$  is the ground-to-level height of floor  $i$ ,  $N$  is the number of stories in the structure,  $b_w$  is the width of the entire strongback bay, and  $b_x$  is the width of the portion of the bay containing the BRBs.

The overturning moment caused by the applied forces is given by Eq. 8:

$$M_r = \gamma \sum_{i=1}^N f_i h_i \tag{8}$$

Satisfying  $M_n \geq M_r$  thus results in the following expression for the required area:

$$A_{sc} \geq \frac{\gamma \sum_{i=1}^N f_i h_i}{\sum_{i=1}^N X_i h_i + Y_i (b_w - b_x)} \tag{9}$$

The resulting design uses the greater of the resulting demand from pushing the frame to the left and pushing it to the right.

Advantages of this method are that it is applicable to general configurations of BRBs. It can also be extended to account for secondary yielding mechanisms such as flexural yielding of beams by including the plastic moment in the free body diagram of the strongback. However, since the design is based on the formation of a plastic overturning mechanism, additional checks may be necessary to ensure acceptable performance (e.g., essentially elastic) for wind loads or frequently occurring earthquakes. Nonetheless, this method has promise and should be further evaluated. Most importantly, an appropriate value of the factor  $\gamma$  must be determined and analyses must confirm that the method results in designs that provide consistent collapse safety. This work presents preliminary analyses to this end.

### 3. Methods

To evaluate the BRB sizing methods described above, strongback braced frames of various configurations were designed for a 4-story prototype building. To isolate the effect of BRB size, frame elements other than the braces were modeled with high stiffness, essentially rigid, elastic elements. The frames were then analyzed as simple 2D OpenSees models using both static pushover analyses and dynamic response history analyses.

#### 3.1 Prototype Building

The building evaluated in this work is the 4-story archetype developed by Simpson (2018), with two strongback braced frames in each direction of loading. The relevant properties of the building are shown in Table 1, and the general frame geometry is shown in Fig. 3. The frames were designed for the FEMA P695  $D_{\max}$  seismic demand category (FEMA 2009).

Table 1: Prototype Building Parameters

| Parameter   | Value |
|---|-------|
| Story weight, 1 <sup>st</sup> (kip)                     | 1812  |
| Story weight, 2 <sup>nd</sup> and 3 <sup>rd</sup> (kip) | 1794  |
| Story weight, roof (kip)                                | 1921  |
| Fundamental period, $T$ (s)                             | 0.939 |
| ELF base shear, $V$ (kip)                               | 292   |
| MCE spectral demand, $S_{MT}$ ( $g_0$ )                 | 0.958 |

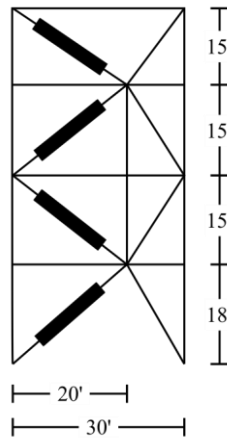


Figure 3: Strongback frame from Simpson (2018)

#### 3.2 Frame Configurations and Other Variables

The prototype building was investigated for several different frame configurations, design options, and with and without geometric nonlinearity (i.e.,  $P-\Delta$  effects).

Four brace layouts are considered, shown in Fig. 4. The standard “X” configuration has a full complement of BRBs, one per story in alternating orientations. Three alternative layouts are considered. The “O” and “E” configurations have braces in every other story, at odd and even stories, respectively. The “S” configuration has a single large brace in the first story.

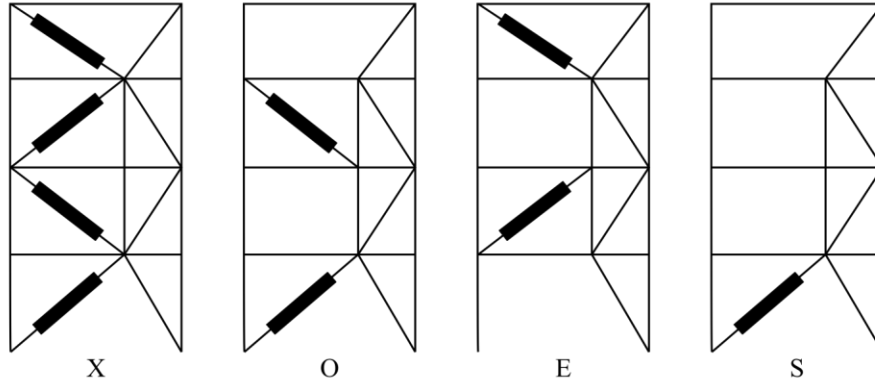


Figure 4: Frame configurations

BRBs were designed using the various methods described in Section 2 for each of the frame configurations. As the proportional shear and constant shear methods are only rational for the X configuration, they were not used to design O, E, or S configuration frames. A total of 10 frames were designed and are presented in Table 2. The frames designed using the equivalent lateral force procedure used the numerical model described in the following section to determine demands in the braces. The initial brace sizing was determined from the relative story shears and a demand-to-capacity ratio of 0.95 was targeted.

Table 2: Designed BRB sizes

| Name | Brace Layout | Design Method                 | 1 <sup>st</sup> story<br>(in. <sup>2</sup> ) | 2 <sup>nd</sup> story<br>(in. <sup>2</sup> ) | 3 <sup>rd</sup> story<br>(in. <sup>2</sup> ) | 4 <sup>th</sup> story<br>(in. <sup>2</sup> ) |
|------|--------------|-------------------------------|--|--|--|--|
| XP   | X            | Proportional shear            | 10.4   | 8.8  | 7.0  | 4.2  |
| XC   | X            | Constant shear                | 7.9  | 7.9  | 7.9  | 7.9  |
| XO   | X            | Overturing ( $\gamma = 3.0$ ) | 8.6  | 8.6  | 8.6  | 8.6  |
| EO   | Even stories | Overturing ( $\gamma = 3.0$ ) | —  | 17.7   | —  | 17.7   |
| OO   | Odd stories  | Overturing ( $\gamma = 3.0$ ) | 16.8   | —  | 16.8   | —  |
| SO   | Single       | Overturing ( $\gamma = 3.0$ ) | 35.0   | —  | —  | —  |
| XE   | X            | Equivalent lateral force      | 3.9  | 3.0  | 2.4  | 1.4  |
| EE   | Even stories | Equivalent lateral force      | —  | 7.5  | —  | 3.6  |
| OE   | Odd stories  | Equivalent lateral force      | 6.4  | —  | 4.0  | —  |
| SE   | Single       | Equivalent lateral force      | 10.0   | —  | —  | —  |

### 3.3 Numerical Model

The numerical model of the structure was built in the OpenSees finite element framework. A schematic of the model is shown in Fig. 5. Analyses were performed in two dimensions of a single strongback frame representative of half the building. Elastic beam elements with high stiffness ( $EA = 10^{10}$  kips,  $EI = 10^{12}$  kip-in.<sup>2</sup>) were used for the strongback. Elastic truss elements with high stiffness ( $EA = 10^{10}$  kips) were used for the beams, columns, and leaning columns. The BRBs were modeled with truss elements with an axial force-displacement relationship calibrated to experimental data and including the effects of low-cycle fatigue (Simpson 2018). Geometric nonlinearity was included at the element level using OpenSees' Corotational transformation for beam-column elements and the CorotTruss element for trusses. Mass was lumped at each story on the nodes of the leaning column. Gravity load equal to the seismic weight tributary to the frame at each level was included as point loads on the nodes of the leaning column. Rayleigh damping of 2.5% at periods  $2T_1$  and  $0.2T_1$  was included, where  $T_1$  is the first-mode period determined by eigenvalue analysis of the model.

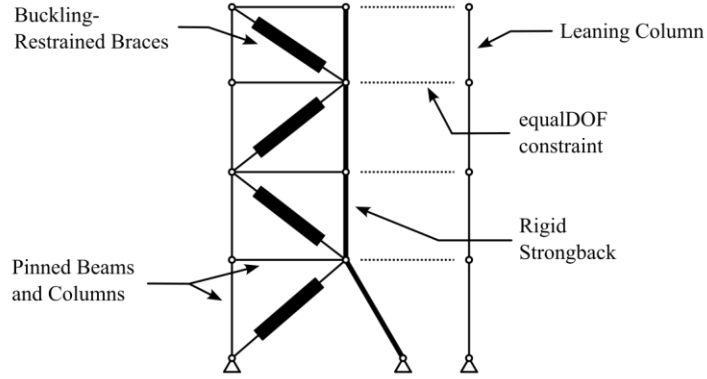


Figure 5: Schematic of the numerical model (X configuration shown)

### 3.4 Analysis Procedure

Static pushover and dynamic response history analyses were performed on all frame configurations.

Pushover analysis was performed using a first-mode proportional distribution of lateral forces

$$f_i \propto m_i \phi_i \quad (10)$$

where  $m_i$  is the lumped story mass at floor  $i$  and  $\phi_i$  is the  $x$ -direction eigenvector for mode 1 at story  $i$  (determined by eigenvalue analysis of the model), until a drop in force of 20% was detected.

Response history analysis was performed using the 22 ground motion pairs from the FEMA P695 far-field set (FEMA 2009). Incremental dynamic analysis was performed with a step of 0.25 for  $S_T$  until collapse was observed (non-simulated, considered to occur when the maximum story drift ratio,  $\theta_{\max}$ , exceeds 0.10). The ground motions were scaled according to FEMA P695 Appendix A.

$$\ddot{u}_{g,\text{applied}} = SF_1 \cdot SF_2 \cdot NF \cdot \ddot{u}_{g,\text{recorded}} \quad (11)$$

$$SF_2 = \frac{S_T}{S_{MT}} \quad (12)$$

where  $NF$  is the normalization factor tabulated in FEMA P695 Table A-4D;  $SF_1$  is the scaling factor for anchoring the normalized far-field record set to MCE spectral demand, tabulated in FEMA P695 Table A-3; and  $SF_2$  is the scaling factor to scale the ground motion to the desired spectral intensity  $S_T$ . The maximum absolute story drift ratio,  $\theta_{\max}$ , was recorded from each analysis.

## 4. Results and Discussion

### 4.1 Pushover Analysis

Load-deformation responses from the pushover analyses are shown in Fig. 6. Response was only determined in one direction, i.e., left to right. Summary results from the analyses are listed in Table 3. These results include  $T_1$ , the fundamental period from the model,  $V_{\max}$ , the maximum base shear,  $\delta_u$  is the lateral roof displacement corresponding to a 20% drop in base shear,  $\Omega$  is the ratio of  $V_{\max}$  to the ELF design base shear  $V$  (i.e., the overstrength),  $\delta_{y,eff}$  is the effective yield displacement, and  $\mu_T$  is the period-based ductility. These quantities are defined in FEMA P695 Section 6.3 (FEMA 2009).

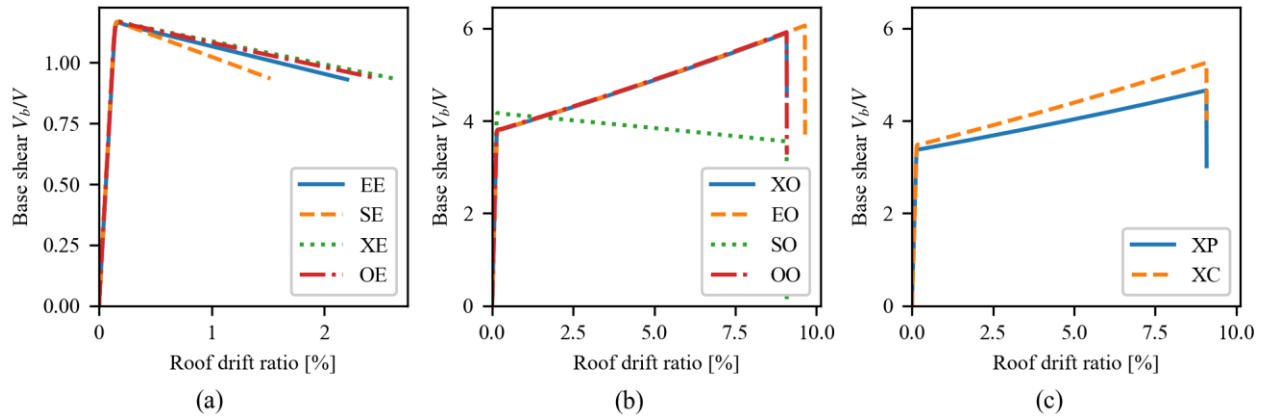


Figure 6: Static pushover curves. Y-axis is normalized by the ELF design base shear  $V$ ; note different scale for (a) due to significantly lower maximum base shear for those configurations

Table 3: Results from pushover analysis

| Name | $T_1$<br>(s) | $V_{\max}$<br>(kip) | $\delta_u$<br>(in.) | $\Omega$ | $\delta_{y,eff}$<br>(in.) | $\mu_T$ |
|------|--------------|---------------------|---------------------|----------|---------------------------|---------|
| XP   | 0.72         | 681                 | 68.7                | 4.66     | 2.25                      | 30.5    |
| XC   | 0.71         | 769                 | 68.7                | 5.26     | 2.54                      | 27.0    |
| XO   | 0.68         | 862                 | 68.7                | 5.90     | 2.85                      | 24.1    |
| EO   | 0.69         | 886                 | 72.9                | 6.06     | 2.93                      | 24.9    |
| OO   | 0.68         | 865                 | 68.7                | 5.92     | 2.86                      | 24.0    |
| SO   | 0.65         | 610                 | 68.7                | 4.17     | 2.02                      | 34.0    |
| XE   | 1.21         | 171                 | 19.7                | 1.17     | 0.73                      | 26.9    |
| EE   | 1.23         | 170                 | 16.6                | 1.16     | 0.73                      | 22.6    |
| OE   | 1.21         | 171                 | 18.7                | 1.17     | 0.72                      | 25.6    |
| SE   | 1.21         | 171                 | 11.5                | 1.17     | 0.72                      | 15.8    |

The designs using the equivalent lateral force method have significantly smaller BRBs than the designs produced using the other methods. As a result, the secondary stiffness of the BRBs was smaller than the stiffness reduction due to  $P-\Delta$  effects, resulting in a negative post-yield stiffness for these frames. Their overstrength was also low in comparison to standard values for BRB frames ( $\Omega_o = 2.5$ , (ASCE 2016)). Conversely, the frames designed using the other methods (i.e., proportional shear, constant shear, and overturning with  $\gamma = 3.0$ ) exhibited high overstrength in comparison to the standard value for BRB frames. Potentially indicating that BRB sizes resulting from these methods are conservative. Frame SO exhibits negative post-yield stiffness which differs from the other frames designed using the overturning method. The single BRB in this

case is subjected to tension. In the nonlinear model, post-yield stiffness is lower for tension than it is for compression. Results from a pushover analysis loading the frame in the other direction would appear different.

#### 4.2 Incremental Dynamic Analysis

The median collapse intensities and per-ground motion spread of collapse intensity is shown in Fig. 7. Individual incremental dynamic analysis results are shown in Fig. 8. The incremental dynamic analysis curve for each ground motion is shown as a grey line. The red solid line indicates the intensity at which half the ground motions cause collapse (i.e., the median collapse intensity  $\hat{S}_{CT}$ ). The black dashed line indicates the intensity of the maximum considered earthquake,  $S_{MT}$ .

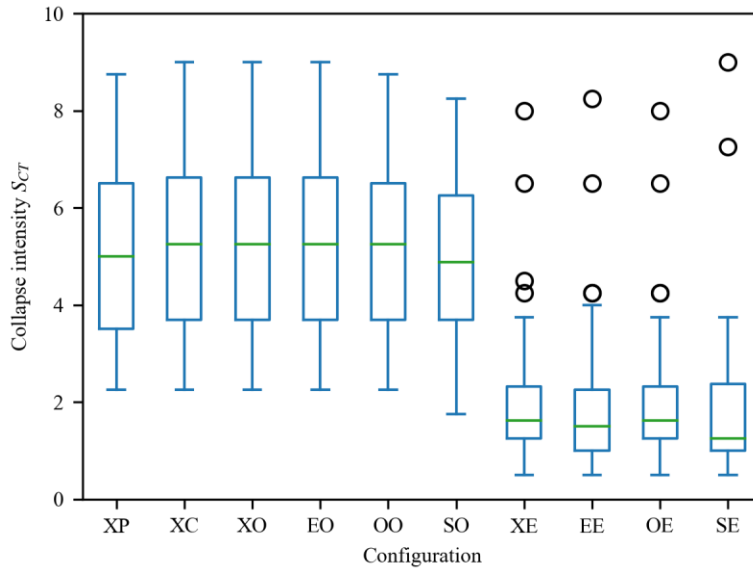


Figure 7: Distribution of collapse intensities from incremental dynamic analysis. Box limits indicate 25<sup>th</sup> and 75<sup>th</sup> percentiles; whiskers indicate data extents up to 1.5 times the inter-quartile range. One outlier ground motion (18b) is not shown for configurations XP through SO, with an  $S_{CT}$  between 15.25 (for frame SO) and 17.75 (for frames XC and XO)

Similar to the pushover analysis results, the largest difference in results is seen when comparing the frames designed using the equivalent lateral force procedure (i.e., XE, EE, OE, SE) and the frames using the other methods (i.e., XP, XC, XO, EO, OO, SO). Within each group, however, the shapes of the incremental dynamic analysis curves are relatively consistent as are the resulting median collapse intensities.

For the non-ELF configurations, the collapse margin ratio ( $CMR$ ), the ratio of  $\hat{S}_{CT}$  to  $S_{MT}$ , is high relative to that from other FEMA P695 studies (FEMA 2009), potentially indicating that these BRB design methods are quite conservative. Adjusted collapse margin ratios ( $ACMR$ ), accounting for system uncertainty and the beneficial impacts of spectral shape, were not computed.

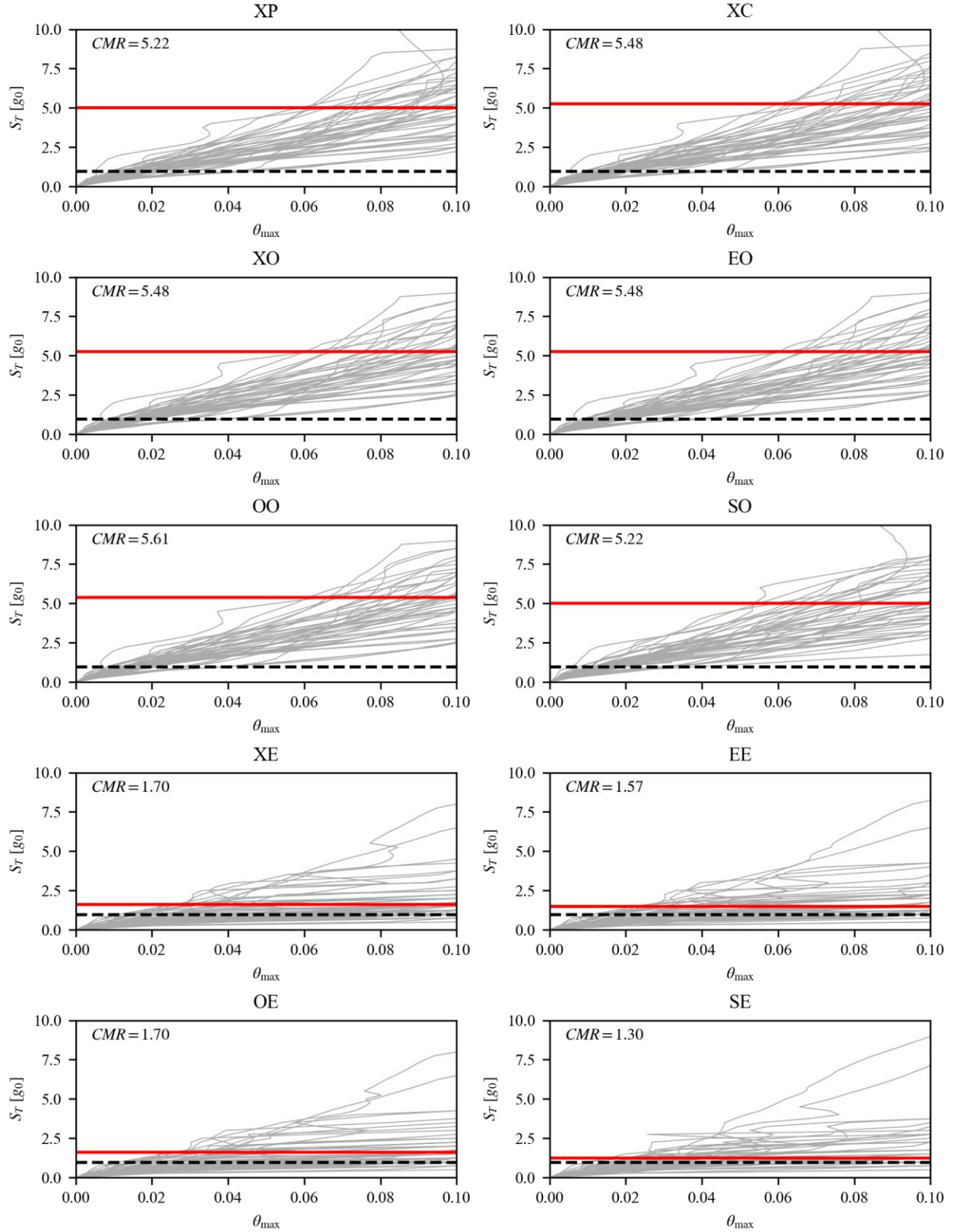


Figure 8: Results from incremental dynamic analysis for each frame configuration. Red solid line indicates median collapse intensity  $\hat{S}_{CR}$ ; black dashed line indicates MCE intensity  $S_{MT}$ ; gray solid lines indicate response from individual ground motions

Of note is that configurations where a full complement of BRBs was not used performed well relative to those where BRBs were used at every level. Single dissipator configurations had slightly lower *CMR* than full-complement and every-other-story configurations, perhaps due to the reduced redundancy or increased asymmetry.

Overall, both the overturning and ELF methods can produce BRB sizes that provide consistent collapse safety margins, though these methods need calibration in order to provide sufficient collapse safety. Further investigation is also needed to determine the spine stiffness and strength necessary to provide the weak story bridging capacity necessary for the range of configurations investigated.

#### 4.3 Investigation of Geometric Nonlinearity and Load Scaling Factor

As a preliminary calibration of the overturning method and to investigate the impact of geometric nonlinearity, additional incremental dynamic analyses were performed using the XO configuration, with the BRB area scaled using different values of the overturning load scaling factor  $\gamma$ . These values and corresponding areas are listed in Table 4. The analyses were performed as described previously with nonlinear geometric transformations and with linear geometric transformations.

Table 4: BRB sizes for XO configuration with varying load scaling factor

| $\gamma$ | $A_{sc}$<br>(in. <sup>2</sup> ) |
|----------|---------------------------------|
| 1.0      | 2.9                             |
| 1.5      | 4.3                             |
| 2.0      | 5.7                             |
| 2.5      | 7.2                             |
| 3.0      | 8.6                             |

The median collapse intensity for each of these configurations, with and without consideration of geometric nonlinearity, is shown in Fig. 9. For  $\gamma = 1.0$ , the geometric nonlinearity is seen to have a major negative impact on the collapse resistance of the frames. For this frame, the post-yield stiffness is negative. For the larger values of  $\gamma$  investigated, geometric nonlinearity is seen to have a modest positive impact on the collapse resistance. This could be the result of a shift in the fundamental period of the structure or the use of a highly simplified analysis model. Nonetheless, the median collapse intensity increases with increasing load scaling factor,  $\gamma$ , indicating that this parameter can be tuned to achieve a target collapse intensity. These results also indicate that it may be beneficial to include overturning demands from  $P$ - $\Delta$  effects in the design procedure for BRB (i.e., in Eq. 8).

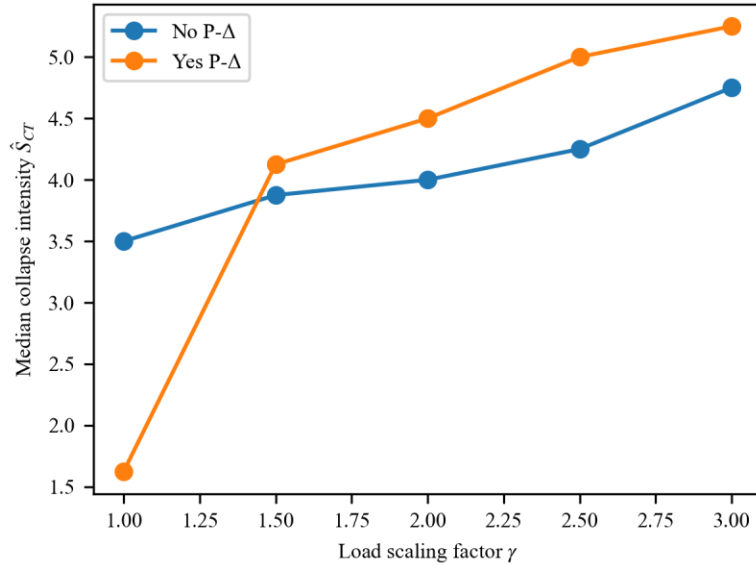


Figure 9: Variation of median collapse intensity  $\hat{S}_{CT}$  of frame configuration XO for multiple values of the load scaling factor  $\gamma$ , with and without geometric nonlinearity

## 5. Conclusions

To investigate a variety of design methods for sizing BRBs in strongback braced frames, a numerical study of a simplified model containing only the essentials of behavior was performed. A method of designing BRBs based on the formation of an overturning plastic mechanism was introduced and compared to other methods for designing BRBs. Static pushover analyses and incremental dynamic analyses were performed to evaluate the impact of the various methods on collapse performance. Preliminary investigation of the necessary scaling factor for the overturning method was performed, as well as investigation of the impact of geometric nonlinearity on the system's resistance to collapse. Key observations from the work include:

- The overturning method can provide a level of collapse safety consistent with other approaches to the design of BRBs in strongback braced frames.
- The overturning method provides a level of collapse safety that is consistent across various arrangements of BRBs within strongback braced frames.
- The load scaling factor,  $\gamma$ , can be tuned to achieve target levels of collapse safety.
- A baseline level of post-yield stiffness may be necessary to provide sufficient collapse safety.

Based on these observations the overturning method described in this work is promising and should be further investigated with more refined models, a larger range of buildings, consideration of demands on the strongback, and secondary energy dissipating elements.

## Acknowledgments

This material is based upon work supported by the National Science Foundation under Grant No. 1940197. Any opinions, findings, and conclusions or recommendations expressed in this material are those of the authors and do not necessarily reflect the views of the National Science Foundation.

## References

- AISC. 2016. *Seismic provisions for structural steel buildings*. Chicago, Illinois: American Institute of Steel Construction.
- ASCE. 2016. *Minimum design loads and associated criteria for buildings and other structures*. Reston, Virginia: American Society of Civil Engineers.
- FEMA. 2009. *Quantification of building seismic performance factors*. Federal Emergency Management Agency.
- Lai, J.-W., and S. A. Mahin. 2014. "Strongback system: A way to reduce damage concentration in steel-braced frames." *Journal of Structural Engineering*, 141 (9): 04014223.
- Panian, L., N. Bucci, and S. Tipping. 2017. "BRBM frames: an improved approach to seismic-resistant design using buckling-restrained braces." *Structures Congress 2017*, 60–71. Denver, Colorado.
- Simpson, B. G. 2018. "Design development for steel strongback braced frames to mitigate concentrations of damage." Ph.D. Dissertation. University of California, Berkeley.